A numerical investigation of the circulation in the Norwegian Sea

By AILEEN CREEGAN, *School of Mathematics, Kingston Polytechnic, Kingston upon Thames, Surrey, England*

(Manuscript received February 18, 1975; in final form February 2, 1976)

ABSTRACT

A numerical model of the Norwegian Sea is developed with the vertical structure modelled by two moving layers. Both the coastline and topography are represented by the finite difference formulation. From such data as is readily available, a preliminary study is made of the relative effects of topography, wind-driving and interaction with the surrounding sea areas in determining the large-scale circulation of the Norwegian Sea.

1. Introduction

The first researches in the Norwegian Sea culminated in 1909 with the publication of 'The Norwegian Sea' by Helland-Hansen and Nansen. Many of their conclusions are still largely accepted, and in particular ideas about the surface circulation pattern have not fundamentally changed. A comprehensive review paper by Lee (1963) describes the state of knowledge at that time, and includes as Fig. 2 a diagram of the surface currents based on Russian and Icelandic investigations. An increasing amount of work has taken place in recent years, although few long term investigations have been carried out, and attention has been concentrated in comparatively limited areas, notably on the channels between the Norwegian Sea and the North Atlantic.

However, despite this fairly clear picture of the surface currents, the principal driving mechanism is still the subject of controversy, being variously ascribed to wind effects (Aagaard, 1970), thermohaline effects (Worthington, 1970), the forcing effects of the North Atlantic Drift component entering chiefly through the Faeroe-Shetland Channel and of the East Greenland Current (Mosby, 1962) and the effect of fresh water run-off from the surrounding land masses (Krauss, 1955). The winds influencing the Norwegian Sea are outside the major semi-permanent wind systems; it is possible that the variability of the wind stress is not consistent with the observed semi-permanent current system being wind-driven. Nevertheless Aagaard (1970), using wind stress data from 1965 to compute monthly mean integrated Sverdrup transports, demonstrates that these are dominated by a cyclonic movement centred on the south–west Greenland Basin and are of a realistic magnitude. He concludes that the wind stress provides an adequate driving mechanism, but also does not doubt the importance of thermohaline effects.

The investigation described here uses a numerical model of the Norwegian Sea in an attempt to reproduce the dominant features of the circulation and to distinguish between the responses to several of the driving mechanisms. The term Norwegian Sea is used to denote the area between Norway and Greenland, bounded to the south by the Greenland-Scotland ridge (about 62° N) and to the north by Spitzbergen (80° N). The area covered by the numerical model is illustrated in Fig. 1.

The major difficulty in such a study lies in obtaining adequate field data. Wind stress distributions and boundary conditions are not available in any systematic form, and it has been found necessary to resort to mean or 'typical' values for many of the input conditions. For a preliminary study of a quasi-

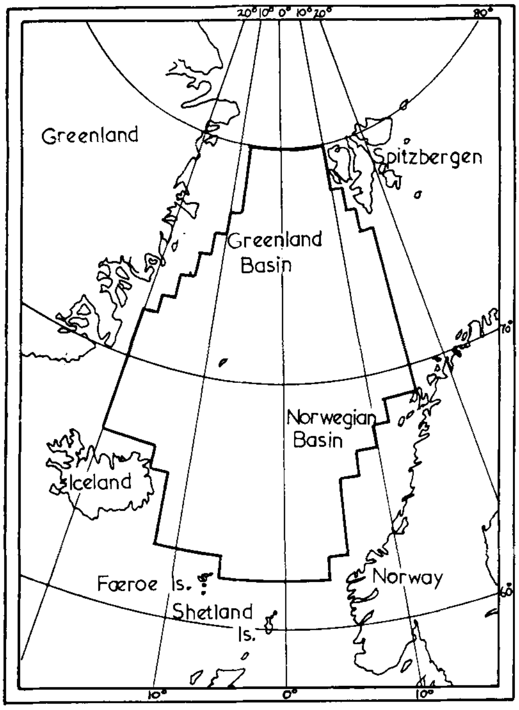

Fig. 1. Map of the Norwegian Sea area indicating the outline of the numerical model.

steady situation, this is felt to be adequate. On this basis, the significance of various parameters in the model and the response to such driving mechanisms as may be incorporated in the model can be tested.

In section 2, the model is discussed in relation to the observational picture of the sea, and section 3 describes the details of the model and input and boundary conditions. The results and conclusions based on test runs of the model are summarised in the last section.

2. The model of the Norwegian Sea

There are considerable topographic variations in the Norwegian Sea, as illustrated for example in Fig. 1 of Lee (1963). The area is split into two main basins, the Norwegian and Greenland Basins, together with the smaller Iceland Basin. The surface circulation consists of two large cyclonic gyres, one in each of the two main basins, together with smaller permanent, semi-permanent and transitory vortices. It seems, therefore, that topography may exert an important controlling influence on the flow pattern.

The main currents are the warm north-flowing Norwegian Current and the cold south-flowing East Greenland Polar Current. Various water masses characterised by distinct salinities and temperatures may be identified within the sea; in general terms however, there is a large mass of approximately homohaline deep water existing below an average depth of 500 m, rather deeper in the east as a result of the surface flowing Atlantic Current as noted by Mosby (1959). Above this interface the mixing of the warm and saline Atlantic water with the colder, fresher water of polar origin does result in spatial density variations, but nevertheless many of the features of the Norwegian Sea may be modelled by a two-layer structure with an average upper layer thickness of 500 m.

The fact that the channels between the various land masses bounding the model area are, on the whole, shallow compared with the depths greater than 3 500 m reached in the main basins lends further support to this model structure. The majority of any inflow or outflow occurring as a result of exchange with the surrounding oceans must take place in the surface layers, and the importance of this may be tested by specifying velocity boundary conditions in the model surface layer to give a particular volume exchange.

There is a difficulty inherent in integrated layered models in that exchange of fluid between layers is not permitted. Thus the cooling and consequent deep water formation in the Greenland Basin cannot be included and hence neither can the overflow of deep water across the various ridges and southwards into the North Atlantic. Moreover, observations indicate this overflow to be of an intermittent nature.

Various authors (e.g. Mosby, 1962; Worthington, 1970; Sukhovey, 1970) have compiled water and heat budgets of the Norwegian Sea. Lee (1963) compares several such budgets and he quotes, for example, figures for the Faeroe–Shetland Channel inflow of between 10.8 and 23.0 km^3 hr^{-1}; more recent estimates generally lie within this range. It is variously suggested that the East Greenland Current flows through the sea interacting little with the interior circulation and that inflow between the Faeroes and Iceland is negligible relative to that in the

Faeroe–Shetland Channel. Sukhovey (1970) questions this latter conclusion, and suggests on the basis of current meter records that the transport estimates in all the channels may be uniformly low. She quotes a minimum of 20 $km^3 hr^{-1}$ in the Faeroe–Shetland Channel. With such variations in mind, for a preliminary study the specified inflow distribution can at best use reasonable figures based on these estimates. For the purposes of this investigation, in order to discover the effect of inflow on a basic wind-driven circulation, the following simple hypothetical situation is considered: Total inflows of 10 and 20 km^3 hr^{-1} through the Faeroe–Shetland Channel are balanced by a corresponding outflow distributed between Greenland and Spitzbergen, so that the magnitude of total transport into each upper layer grid square on the boundary is prescribed. As suggested above, the East Greenland Current is neglected; further justification for this is that it is largely confined to shelf areas off Greenland excluded from the model.

3. The numerical model

Based on the foregoing considerations, the Norwegian Sea is modelled by a two-layer structure, integrated in depth across each layer. The formulation enables the response to wind-driving, bottom topography and exchange with surrounding sea areas to be incorporated, together with a consideration of the effect of bottom and interface friction coefficients and of the density difference between the layers, but it ignores thermohaline effects. The model outline is shown in Fig. 1 and approximates to the 500 m depth contour over the continental shelf.

The most straightforward way of setting up the model is to use an explicit finite difference scheme, which readily permits the inclusion of an irregular boundary and topography. Since the area to be considered is large and at high latitudes, the grid points are chosen at regular spacings of latitude and longitude. The coordinates are defined with x eastwards, y northwards and z vertically upwards, so that the Δx grid spacing decreases towards the north. u and v are the corresponding velocity components. A 'staggered' grid configuration has been used; the boundary is defined so that u-points lie along east and west-facing coasts, v-points

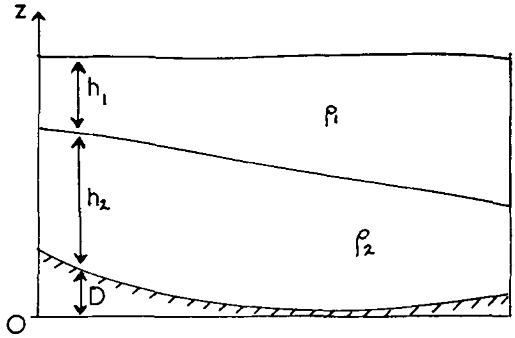

Fig. 2. Vertical structure of the layers in the numerical model.

along north and south-facing coasts in order that boundary conditions of no normal flow (at a coast) or a specified flow (at an open boundary) may be satisfied. Layer thicknesses are evaluated entirely at interior points. The vertical structure of the model is shown in Fig. 2 and the subscripts 1 and 2 denote quantities in the upper and lower layers respectively.

Various approximations are made in obtaining the equations in the final difference form. The pressure is assumed to be given by the hydrostatic approximation, lateral friction is assumed to be negligible compared with vertical friction, the interface and bottom stresses $\boldsymbol{\tau}_I$ and $\boldsymbol{\tau}_B$ are taken as proportional to the relative velocity vetween layers at any interface, i.e. $\boldsymbol{\tau}_I = \alpha\varrho_2(\mathbf{u}_1 - \mathbf{u}_2)$, $\boldsymbol{\tau}_B = \alpha'\varrho_2\mathbf{u}_2$, and the approximation $1/\varrho_1 \triangleq 1/\varrho_2$ is used. The densities of the two layers are related by $\varrho_1 = \varrho_2(1 - \bar{\varrho})$.

Subject to these approximations, if the (linear) equations of motion and the continuity equation are integrated across each layer, the resulting system of equations is:

$$\frac{\partial u_1}{\partial t} - fv_1 = -g(h_1 + h_2 + D)_x + \frac{\tau^x}{\varrho_2 h_1} - \frac{\alpha}{h_1}(u_1 - u_2),$$

$$\frac{\partial v_1}{\partial t} + fu_1 = -g(h_1 + h_2 + D)_y + \frac{\tau^y}{\varrho_2 h_1} - \frac{\alpha}{h_1}(v_1 - v_2),$$

$$\frac{\partial u_2}{\partial t} - fv_2 = \bar{\varrho} g h_{1x} - g(h_1 + h_2 + D)_x + \frac{\alpha}{h_2}(u_1 - u_2) - \frac{\alpha'}{h_2}u_2,$$

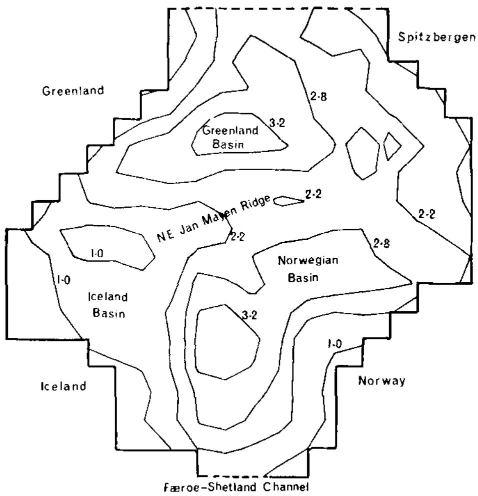

Fig. 3. Computer plot of the model area showing the main topographic features. Depths are in kilometres. Dotted lines indicate regions of open boundary.

$$\frac{\partial v_2}{\partial t} + fu_2 = \bar{\varrho}gh_{1y} - g(h_1 + h_2 + D)_y + \frac{\alpha}{h_2}(v_1 - v_2)$$

$$-\frac{\alpha'}{h_2}v_2,$$

$$\frac{\partial h_1}{\partial t} + \frac{\partial}{\partial x}(h_1 u_1) + \frac{1}{\cos\theta}\frac{\partial}{\partial y}(h_1 v_1 \cos\theta) = 0,$$

$$\frac{\partial h_2}{\partial t} + \frac{\partial}{\partial x}(h_2 u_2) + \frac{1}{\cos\theta}\frac{\partial}{\partial y}(h_2 v_2 \cos\theta) = 0$$

where θ is the latitude, f is the Coriolis parameter and $\boldsymbol{\tau} = (\tau^x, \tau^y, 0)$ is the surface stress (independent of t).

The equations are marched forward in time using forward differences in time and centred differences in space. Where a quantity is not available at the required point, a simple averaging process is used, and in particular for the Coriolis term values of velocity at four surrounding points are used. The stability requirement for such a numerical scheme is essentially the Courant–Friedrichs–Levy criterion for stability of the wave equation, namely

$$\left(\frac{\Delta x_{\min}}{\Delta t}\right) \geqslant (2gh_{\max})^{1/2}.$$

The system of equations is integrated starting from rest and with $h_1 = 0.5$ km at $t = 0$. With mesh points defined in terms of latitude and longitude (θ, ϕ),

$$\Delta x_j = R\cos\theta_j \Delta\phi, \quad \Delta y = R\Delta\theta$$

where the subscript j denotes variation with latitude and $R = 6\,000$ km is the earth's radius. For spacings between *like* grid points defined by $\Delta\theta = 1°$, $\Delta\phi = 2°$ then $\Delta y = 104.72$ km and Δx(north) $= 36.37$ km, Δx(south) $= 98.33$ km. Other values are $\varrho_2 = 1.028 \times 10^{12}$ kg km^{-3}, $\varrho_1 = 1.026 \times 10^{12}$ kg km^{-3}, $\Delta t = 0.05$ hr (3 min), while several values for the interface and bottom friction were tested in the model.

Detailed information on the bathymetry of the sea was derived from a 1963 bathymetric chart of the Norwegian Sea and the wind stress data were estimated from Aagaard (1970) Fig. 3 shows the model area as represented on computer plots and indicating the main topographic features and Fig. 4 illustrates diagrams of the wind stress vectors for the arrays used in the computations. (The graphical programs plot values at regular spacings and so cause distortion due to the curvature of the earth.)

The bottom topography is defined in such a way that it may be multiplied by a scaling factor in an investigation of the effect of topography on the circulation. Although stratification is partially modelled by the two layer structure, the large part of the volume is occupied by the homogeneous lower layer. It is well known that homogeneous models enhance the effect of topography and Galt (1973) reports that a much reduced topographic effect gave the best agreement with reality in a one-layer model of the Arctic. This result applies also to the two-layer model, although the fact that the deep velocities are somewhat smaller than in the surface layer reduces the effect. However, no computational difficulties arise until the topographic effect approaches 100% of the true size. In this case, as the interface level adjusts during the spin-up process, the lower layer depth vanishes at certain points and the integration cannot be continued.

The results which are illustrated here show the circulation after a 24 day integration, although longer (36 day) integrations revealed no significant difference in the flow pattern and little further energy increase. Accordingly, the 24 day integrations were accepted as showing the main characteristics of the circulation. In

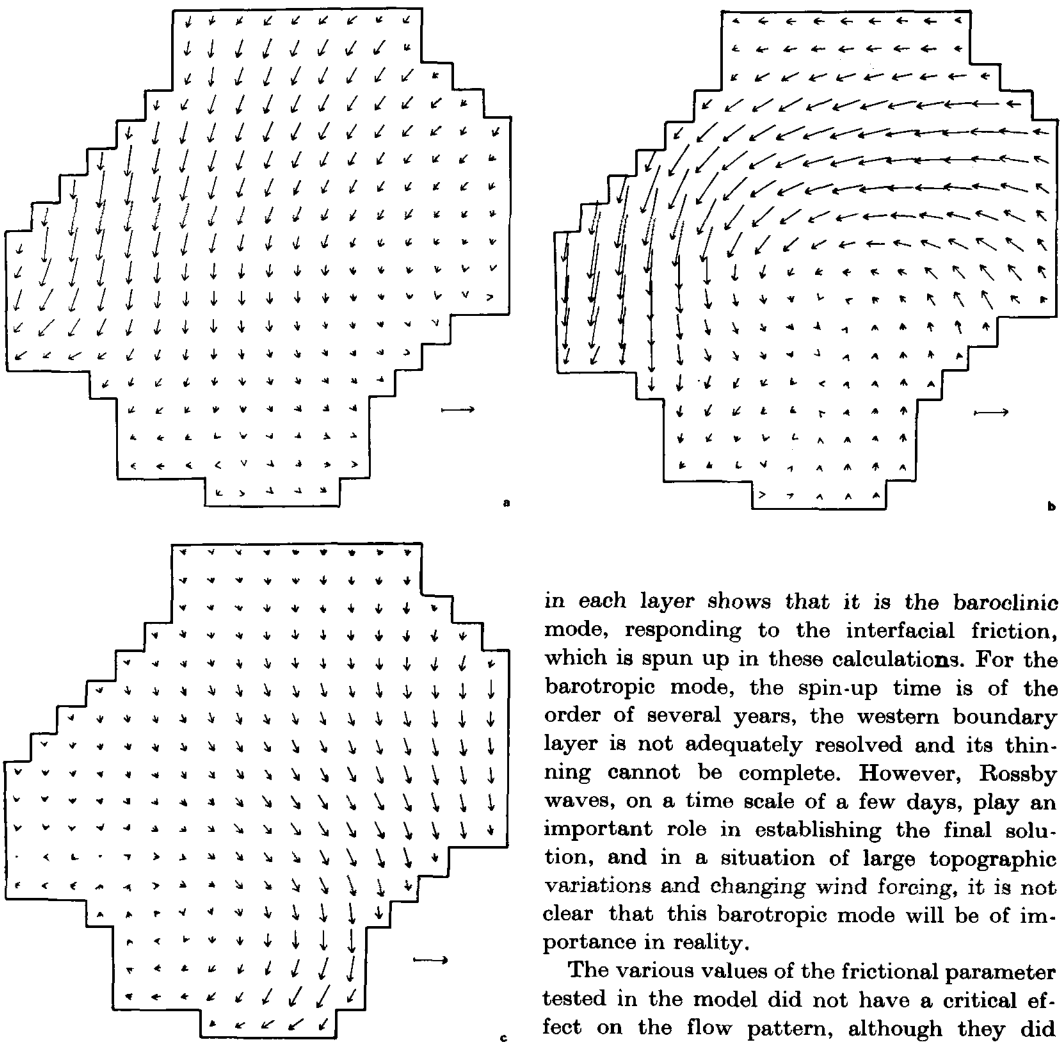

Fig. 4. Computer plots of applied surface wind stress. Arrow scale represents 15×10^9 kg km^{-1} hr^{-2}. Stress distributions apply to 1965 and are (*a*) annual mean, (*b*) September mean, (*c*) July mean stresses.

addition, some wind stresses used are monthly mean values and the sea is spun-up to show the response to each stress distribution; weather patterns in the area are likely to exist on a time-scale of 1–3 weeks and so integrations of this length will be useful in assessing the resultant circulation.

I am grateful to a referee for a useful discussion of the following modal analysis: The method of normal modes (as used by Nowlin (1967)) applied to the equations of vorticity balance in each layer shows that it is the baroclinic mode, responding to the interfacial friction, which is spun up in these calculations. For the barotropic mode, the spin-up time is of the order of several years, the western boundary layer is not adequately resolved and its thinning cannot be complete. However, Rossby waves, on a time scale of a few days, play an important role in establishing the final solution, and in a situation of large topographic variations and changing wind forcing, it is not clear that this barotropic mode will be of importance in reality.

The various values of the frictional parameter tested in the model did not have a critical effect on the flow pattern, although they did affect the degree of damping and boundary layer width. The actual value for all the results presented here is $\alpha = 5\ \alpha' = 0.0005$ km hr^{-1}, which is close to the value used by Nowlin (1967).

4. Results and discussion

Figs. 5–11 are the computer plots of surface circulation for a representative sample of the results obtained. Where topography is included, it is taken as 30% of the actual topography.

Pressure measurements over the Norwegian Sea indicate that the prevailing wind conditions give a cyclonic distribution of wind stress over

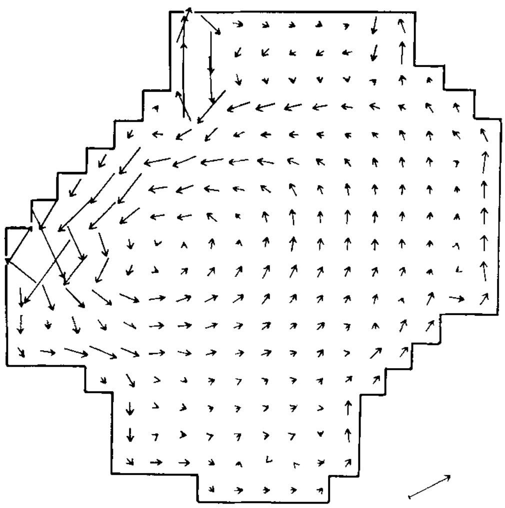

Fig. 5. Depth-mean velocity vectors, centred on grid points, resulting from stress 4*a* in the absence of topography and with closed boundaries. Arrow scale represents 5 cm s^{-1}.

the area, and this is reflected in the annual mean (Fig. 4*a*) and most monthly mean (e.g. Fig. 4*b*) stresses. However, certain monthly mean stresses may show a reversal of this tendency (e.g. Fig. 4*c*).

In Fig. 5 the circulation is driven by the stress shown in Fig. 4*a* in the absence of topography and with closed boundaries. Thus the wind stress curl is positive everywhere except near Iceland and in the extreme northwest. There is good agreement with the Sverdrup transport calculation of Aagaard (1970), with the expected westward intensification on a β-plane giving a cyclonic gyre centred on the SW Greenland Basin and a broad northwards flow across the Norwegian Basin. There is, however, no indication of the separation into two distinct cyclonic gyres in the region of the two main basins. The flow exhibits a strong response to anomalously large negative values of wind stress curl near the western boundary. The corresponding flow in the lower layer is similar but somewhat weaker.

If the topographic effect is now included, the result is rather dramatic, as shown in Fig. 6. There is a reduction in intensity and at first sight little structure in the resulting flow. This decrease in flow is also reported by Galt (1973) for a one-layer model. The dotted lines are depth contours to indicate the areas of the two main basins. Many of the features previously present are now entirely absent, notably the main gyre and western boundary current. Topography must be exerting a strong controlling influence on the flow, and indeed the main discernible feature is a generally cyclonic flow around the Norwegian Basin which follows closed f/H contours. Closed f/H contours are less in evidence in the Greenland Basin, which is a likely reason for the difference in flow between the two main basins. In the far north, the topographic effect reinforces the β-effect and so the top few rows of velocity vectors are similar to the previous case.

Thus although the inclusion of topography breaks down the single gyre found in fig. 5, it does not result in a circulation particularly close to that observed, and nor is the flow of a realistic magnitude. The next question to be asked is whether adding the North Atlantic inflow will augment the wind-driven circulation to give a better agreement with observations. Fig. 7 shows the effect of including the simple exchange situation described in section 3. The inflowing water has only a northward velocity component and is directed along f/H contours, both to east and west. The eastward part joins the Norwegian gyre and skirts the Norwegian Basin in a fairly broad flow. There is a narrow current following f/H contours up and out past West Spitzbergen. The westward branch is of

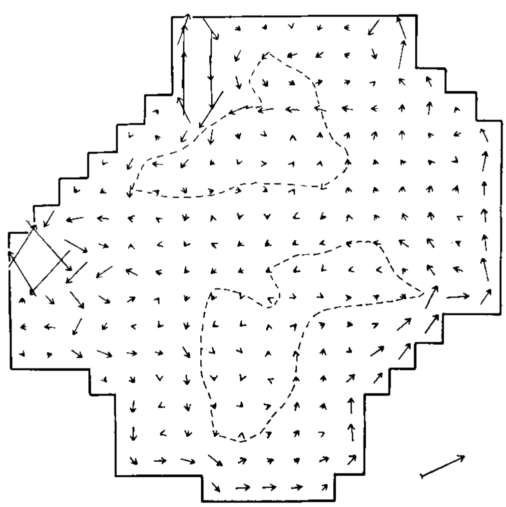

Fig. 6. Equivalent calculation to 5 with 30% topography included. Dotted contours indicate the areas of the two main basins.

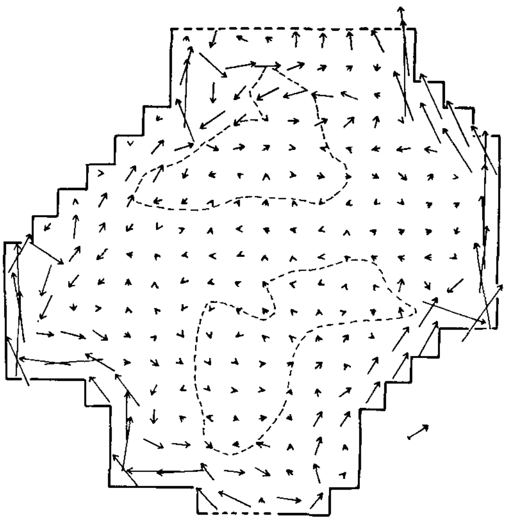

Fig. 7. Equivalent calculation to 6 with open boundaries (denoted by the broken line). Total volume of inflow through the Faeroe–Shetland Channel is 20 km^3 hr^{-1}. Arrow scale represents 5 cm s^{-1}.

greater interest, as it opposes the general cyclonic wind-driven circulation; although there is evidence of a little being swept back into the Norwegian gyral, the majority persists up the Greenland coast. These stronger currents are not reflected in the lower layer circulation, which does not show any marked differences from the previous case. These results, of course, refer to velocity vectors only and can mask significant transport variations. In this case, for the first time in the results discussed here, there are considerable (>10 m) variations in the level of the interface. Under the influence of the Atlantic current up the Norwegian coast, the interface level moves downward by up to 50 m and upward by a similar amount at the western boundary during spin-up. Thus despite the suggestion from the upper layer velocity vectors of no obvious preference for east or west, there is a much greater transport up the Norwegian coast.

The view expressed by Sukhovey (1970) of considerable recirculation occurring near the Faeroe–Shetland Channel with some of the Atlantic water re-entering the ocean between Iceland and Faeroes is rather attractive in explaining these results. They suggest that, to fit with the observed circulation there should be an outflow, possibly nearing 50% of the Faeroe–Shetland inflow, taking place to the east of Iceland. This will clearly need a good data set from measurements in the various channels to use as input to the model. It is worth noting here that although the distribution of outflow near Spitzbergen has been prescribed in a rather arbitrary manner for lack of observational results, varying this distribution has only local effects on the flow. With all these open boundaries it seems probable that the boundary conditions will vary according to the atmospheric forcing over large areas.

Before drawing tentative conclusions about the results of the model, the next four figures show the results from repeating the last two model runs for the wind stresses 4*b* and *c*.

In Fig. 4*b* the wind stress shows a strong cyclonic distribution with positive curl except near Spitzbergen where it is small and negative. In the absence of topography the anticipated single strong cyclonic gyre is obtained. Fig. 8 shows the upper layer flow when topography is present, with cyclonic flow following f/H contours round both basins, although the Norwegian gyre is much the stronger. In Fig. 9, where inflow is included, the Norwegian Current is the dominant feature, but again there is a westwardflowing branch which counteracts much of the cyclonic flow. Thus even with a strong cyclonic wind stress including the effect of recirculation near the Faeroes seems likely to improve the flow pattern.

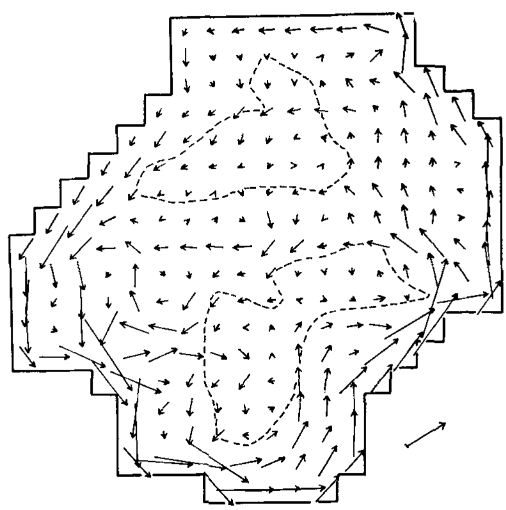

Fig. 8. Upper layer flow from stress 4*b* with closed boundaries and 30% topography.

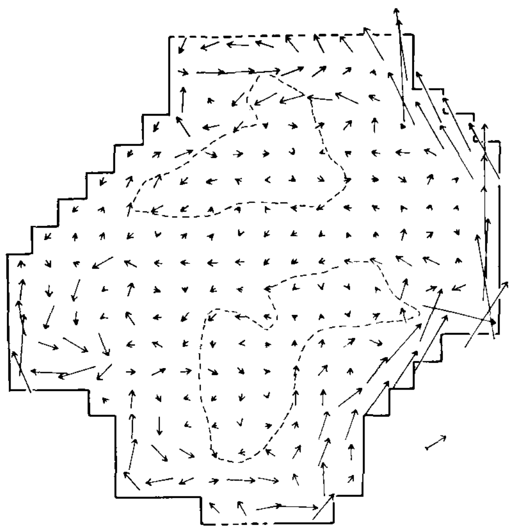

Fig. 9. Equivalent calculation to 8 with open boundaries.

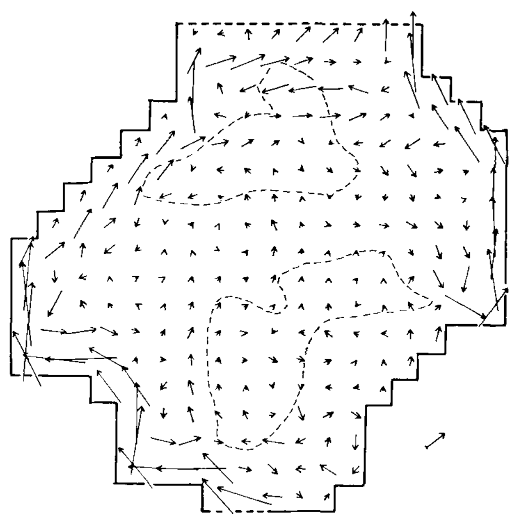

Fig. 11. Equivalent calculation to 10 with open boundaries.

For the stress in Fig. 4*c*, there is a smaller and generally negative wind stress curl except for some positive values near the Barents Sea. The results (Fig. 10) with only topography and wind stress show the anticyclonic circulation pattern which might be anticipated. Including inflow (Fig. 11), the anticyclonic flow has largely inhibited the Norwegian Current, although there is still a drop in the interface there. Further north there is a coastal current derived from water in the Norwegian gyre.

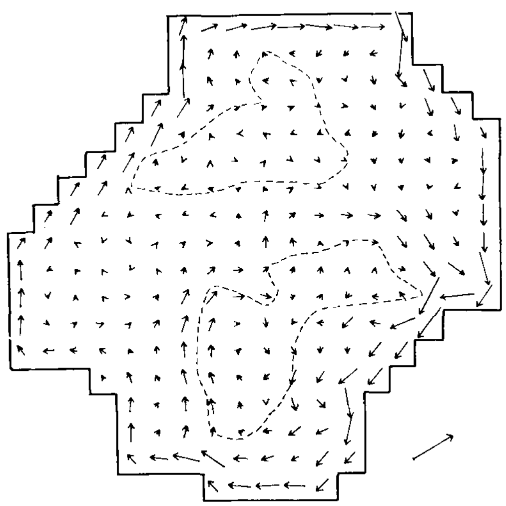

Fig. 10. Upper layer flow from stress 4*c* with closed boundaries and 30 % topography.

The difficulty in obtaining reliable input data has strictly curtailed the scope of this investigation, and far more detail in wind stress and source distribution and in their time dependence is needed. The greater resolution provided by reducing the grid spacing does not seem of value until such information is available. Nevertheless, the preliminary results obtained do indicate in which areas additional data are likely to be most critical. A further factor to be taken into account is the partial ice cover in winter. Galt (1973) discusses how the surface stress conditions are modified by pack ice in relation to the sign of the wind stress curl.

Accepting the accuracy of the standard diagrams representing the residual circulation of the surface waters, the following conclusions about the relative importance of the driving forces based on the results of this model are proposed. The observed circulation is difficult to explain in a wholly wind-driven flow; absence or reversal of the main currents is not observed, although clearly such a situation could well occur if anticyclonic stresses occurred for more than a few weeks. Still, the average effect of the wind is to produce a general cyclonic circulation within the Norwegian Sea, and for any given stress distribution, the topography serves to split the resultant circulation into two gyres, with that in the Norwegian Basin being the more pronounced. What is evident is that inflow effects cannot be neglected when considering driving mechanisms. Even with the over-simplification of this model certain features become apparent, especially the more realistic magnitudes for the velocities and the flow and corresponding interface displacement along the eastern boundary. To progress further, more accurate modelling is required, particularly with regard to the details of the exchange with the Atlantic and inclusion of the East Greenland Polar Current. Nevertheless, there is a clear implication that the effect of inflow is to establish a more permanent current system than could be expected from the wind stress alone.

REFERENCES

Aagaard, K. 1970. Wind-driven transports in the Greenland and Norwegian Seas. *Deep Sea Res.* *17*, 281–291.

Galt, J. A. 1973. A numerical investigation of Arctic Ocean dynamics. *J. Phys. Oceanogr.* *3*, 379–396.

Krauss, W. 1955. A contribution ot the system of ocean currents in the higher latitudes. *Deut. Hydrogr. Zeit.* *8*, 102–111.

Lee, A. 1963. The hydrography of the European Arctic and Subarctic seas. *Oceanogr. Mar. Biol. Ann. Rev.* *1*, 47–76.

Mosby, H. 1959. Deep water in the Norwegian Sea. *Geophysica Norvegica* *21*, 1–61.

Mosby, H. 1962. Water, salt and heat balance of the North Polar Sea and of the Norwegian Sea. *Geophysica Norvegica* *24*, 289–313.

Nowlin, W. D., Jr. 1967. A steady, wind-driven, frictional model of two moving layers in a rectangular ocean basin. *Deep Sea Res.* *14*, 89–110.

Sukhovey, V. F. 1970. An investigation of the water exchange between the Atlantic and Arctic Oceans based on instrumental observations. *Morsk. Gidrofiz. Issled.* *49*, 125–146.

Worthington, L. V. 1970. The Norwegian Sea as a mediterranean basin. *Deep Sea Res.* *17*, 77–84.

ЧИСЛЕННОЕ ИССЛЕДОВАНИЕ ЦИРКУЛЯЦИИ В НОРВЕЖСКОМ МОРЕ

Разработана численная модель Норвежского моря с вертикальной структурой, моделируемой двумя движущимися слоями. Как береговая линия, так и топография представлены конечно-разностной формулировкой. На этой основе выполнено предварительное исследование относительных эффектов топографии, роли ветра и взаимодействия с окружающими морями крупномасштабной структуры циркуляции Норвежского моря.